



Numerical Study of a Passive Scalar Transport from Thermal Power Plants to Air Environment

A. Issakhov^(✉) and A. Baitureyeva

Al-Farabi Kazakh National University,
71, al-Farabi Avenue, 050040 Almaty, Republic of Kazakhstan
alibek.issakhov@gmail.com, abatur@yandex.kz

Abstract. This paper presents computational fluid dynamics (CFD) techniques in modeling the pollution distribution from thermal power plant. Carbon dioxide (CO_2) dispersion from a thermal power plant was simulated. The mathematical model and numerical algorithm were tested using a test problem and gave a good match with the experimental data. The influence of gravity force was taken into account. The k-epsilon model of turbulence with the buoyancy force was used. Calculations were performed by ANSYS Fluent. As a result, there was found a distance from the source at which the impurity settles on the ground surface.

Keywords: Navier-Stokes equations · Mass transfer · Numerical simulation · Air pollution · Concentration

1 Introduction

Energy is the most significant among the industries that have a negative impact on the environment. This is due to the fact that the development of society and the population growth constantly require more and more energy. As a consequence, emissions of pollutants into the atmosphere should also increase. Therefore, studying the nature of these emissions, their structure, the impact of these pollutants on the elements of the environment - is one of the urgent tasks of modern applied ecology. The structure of pollution emissions into the atmosphere depends on the capacity of emission sources, the location of energy facilities in relation to ecologically significant areas, and the physical nature of emissions. For example, discharges from the coal industry and from TPPs are close in magnitude, but they substantially exceed the discharges from the gas industry. NPPs shed much less sulfates, chlorides and nitrates than TPPs, but more phosphorus emits out of nuclear power plants. In addition, it should be noted that mercury, selenium, fluorine and other elements, that are not completely captured by the waste gas filtration system, become a source of air pollution in coal combustion products at high-capacity power plants (over 2 million kW). Volatile (lead, copper, zinc, cerbium, itterium, etc.) elements are distributed between solid combustion products, which requires special procedures for the disposal of ash and

slag wastes. In addition, the nature of the impact on ecological systems depends on the natural conditions of the location area and the physical nature of the ejected ingredient. Recently, much attention has been paid to the effects of various pollutants on environmental and human elements, as well as on models and physical principles of the spread of these pollutants in environmental objects.

At the same time, the issues of the emissions spread and their impact on ecological systems have not been adequately worked out. The most successful is the assessment of the effect of thermal emissions and discharges on the thermal regime of rivers and reservoirs. However, the study of thermal emissions and the associated effects of changing microclimatic conditions, impact on terrestrial ecological systems, require further elaboration taking into account the concepts of sustainable ecological development of ecosystems, monitoring systems and environmental safety. The purpose of this work is to assess the impact of large-scale energy emissions on the environment based on a numerical model of emissions diffusion from sources. One of the pipes of Ekibastuz SDPP-1 (Kazakhstan) was chosen as the real object of the research. Its height of stack is 330 m and the diameter is 10 m.

2 Mathematical Model

A detailed description of the latest works about the study of the jet distribution in the crossflow is given in [1] and [2]. The velocity field is numerically calculated in papers [3–7]. The passive scalar mass fraction field was considered in papers [8–10]. CFD is often used to solve these problems. Reynolds-averaged Navier-Stokes equations (RANS) were used and the results were compared with the experimental data in papers [11–16]. Good correspondence between numerical solutions (DNS) and experiments was obtained by [17] and [18]. However, the DNS simulation requires large computational costs, which is unacceptable for solving large-scale problems in real scales [1] and [19–23]. As a result, the k-epsilon turbulence model was used in this paper. The CFD simulations of such processes are based on the resolution of the Navier-Stokes equations (continuity of mass and momentum equations) [24–28]. Since the RANS equation was applied taking into account the buoyancy, the equations for turbulent kinetic energy and dissipation are presented as follows:

$$\frac{\partial k}{\partial t} + \frac{\partial}{\partial x_j}(u_j k) = \frac{\partial}{\partial x_j} \left[\left(\mu + \frac{\mu_t}{\sigma_k} \right) \frac{\partial k}{\partial x_j} \right] + P_k - \rho \varepsilon + P_{kb}$$

$$\frac{\partial \varepsilon}{\partial t} + \frac{\partial}{\partial x_j}(u_j \varepsilon) = \frac{\partial}{\partial x_j} \left[\left(\mu + \frac{\mu_t}{\sigma_\varepsilon} \right) \frac{\partial \varepsilon}{\partial x_j} \right] + \frac{\varepsilon}{k} (C_{\varepsilon 1} P_k - C_{\varepsilon 2} \rho \varepsilon + C_{\varepsilon 1} P_{\varepsilon b})$$

The term P_k represents the generation of turbulence kinetic energy due to the mean velocity gradients. P_{kb} , $P_{\varepsilon b}$ represent the buoyancy forces, where $P_{kb} = -\frac{\mu_t}{\rho \sigma_\rho} \rho \beta g_i \frac{\partial T}{\partial x_i}$ and $P_{\varepsilon b} = C_{3max} (0, P_{kb})$. Here β is thermal expansion coefficient, $\sigma_\rho = 0.9$, C_{s1} , C_{s2} , σ_k , σ_ε are constants. For solving conservation equations for chemical species, ANSYS Fluent predicts the local mass fraction of each species Y_i , through the solution of a convection-diffusion equation for the i -th species.

$$\frac{\partial}{\partial t}(\rho Y_i) + \nabla \cdot (\rho \mathbf{u} Y_i) = -\nabla \cdot \mathbf{J}_i + R_i + S_i$$

Here R_i is the net rate of production of species i by chemical reaction and S_i is the rate of creation by addition from the dispersed phase plus any user-defined sources.

For the turbulent flows, the mass diffusion is computed in the following form:

$$\mathbf{J}_i = -\left(\rho D_{i,m} + \frac{\mu_t}{Sc_t}\right) \nabla Y_i$$

Where $Sc_t = \frac{\mu_t}{\rho D_t}$ - turbulent Schmidt number (μ_t - turbulent viscosity and D_t - turbulent diffusivity).

3 Test Problem

An experimental study for this test problem was conducted in a low speed wind tunnel on a row of six rectangular jets injected at 90° to the crossflow [1, 29] and [30]. Mean velocities were measured using a three-component laser Doppler velocimeter operating in coincidence-mode. Seeding of both jet and cross stream air was achieved with a commercially available smoke generator. To complement the detailed measurements, flow visualization was accomplished by transmitting the laser beam through a cylindrical lens, thereby generating a narrow, intense sheet of light.

3.1 Computational Domain and Grid

The computational domain included the jet channel and the space above the flat plate. A square jet was used in this study and jet diameter (jet width) was D , which was used as the length unit. The origin of the coordinate system was located at the center of the jet exit. The calculation area of the test problem is a three-dimensional channel with the pipe entering into it. The height of the crossflow channel is $20D$, jet channel length is $5D$, the length of the crossflow channel is $45D$, the width is $3D$, and the center of the pipe located at $5D$ from the inlet (See Fig. 1). Number of grid points: main channel $230 \times 100 \times 21$ and jet channel $7 \times 30 \times 7$ nodes. Grid was unstructured, total number of nodes was 533 697 [1].

3.2 Boundary Conditions and Flow Characteristics

The ratio of the jet velocity to the crossflow velocity is denoted by R , and is expressed as:

$$R = V_{jet}/V_{crossflow}$$

In papers [1] and [30] considered various R (0.5, 1.0 and 1.5). In present paper $R = 0.5$ was considered, that is why the jet velocity was 5.5 m/s, crossflow velocity was 11 m/s. Water was chosen as the material of the crossflow and jet

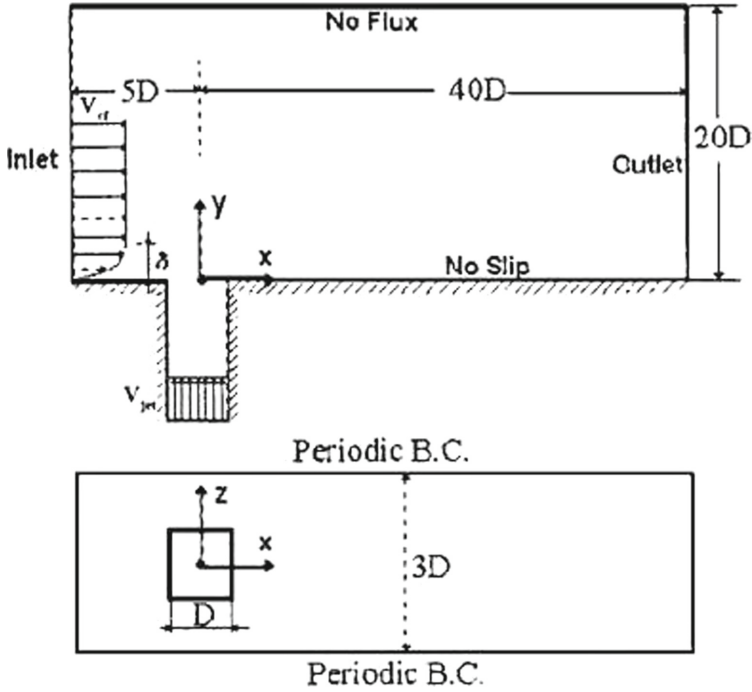


Fig. 1. Configuration of test problem computational domain.

fluid. The jet diameter was $D = 12.7$ mm. Based on the above data, the Reynolds number is defined as:

$$Re_{jet} = \rho V_{jet} D / \mu = 4700$$

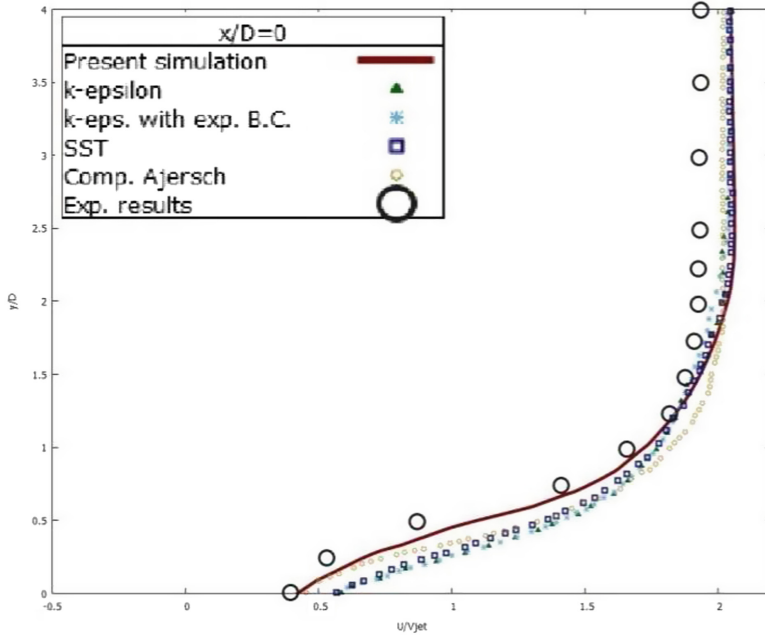
Five types of boundary conditions were used: inlet, outlet, no flux, wall, periodic (See Fig. 1). According to the experimental data, the boundary layer thickness is $2D$. To describe the initial crossflow velocity profile in the boundary layer, $1/7$ power law wind profile was used:

$$\frac{u}{u_r} = \left(\frac{z}{z_r} \right)^\alpha$$

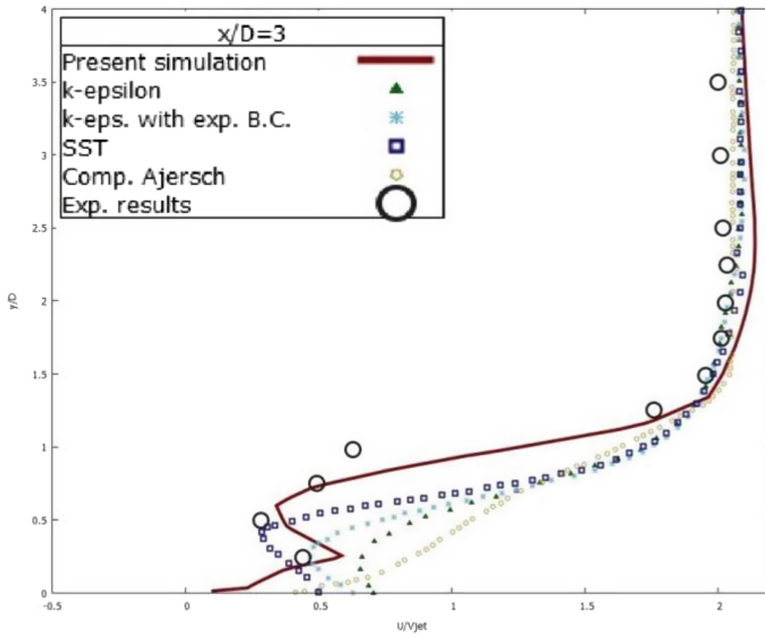
Here u is the wind velocity at height z and u_r is the known wind velocity at a reference height z_r . α is empirically obtained coefficient, which varies depending on the atmosphere stability. Here, $\alpha = 1/7$ for neutral stability conditions. Uniform velocity (11 m/s) was defined above the boundary layer $2D$ [1].

3.3 Comparison of Numerical Results

Figure 2 shows a comparison of the numerical results of present paper with experimental data and computational solutions of other authors ($R = 0.5$). The red solid line marks the results of present paper, round-shaped of experimental data



a)



b)

Fig. 2. Comparison of results for streamwise velocity at jet center plane ($z/D=0$) for $R=0.5$: (a) $x/D=0$; (b) $x/D=3$. (Color figure online)

(See [29]) and the rest lines illustrate computational solutions of other authors (See [30]). The results for the SST model are shown by blue squares. Comparative analysis showed that the k-epsilon model and the SIMPLE algorithm with finite volume method yield closest results to the experimental data (See Fig. 2b) [1].

The solutions obtained in this paper turned out to be more accurate than those computational solutions obtained by other authors ([30]). Values of the red line (u/V_{jet}) at $y/D = 0$ close to zero, when other results close to 0.5–0.7. This is more accurate from a physical point of view, since it is a near-wall field. Moreover, in the interval y/D 0.5–1.5 it is noticeable that the current calculations are much closer to the experimental data than the others. The reason is the quality of the grid: in present paper unstructured grid was used, the number of nodes was 533 697, while in paper [30] used structured grid and the number of nodes was 265 000 [1].

3.4 Geometry, Grid and Boundary Conditions

The computational domain is a three-dimensional box with a pipe inside it (See Fig. 3). The boundary conditions were set analogically to test problem: inlet, wall, outlet, symmetry, periodic. The length of the geometry was 2500 m, the height was 1500 m, the width was 200 m. The pipe was located at 250 m from the entrance of the wind.

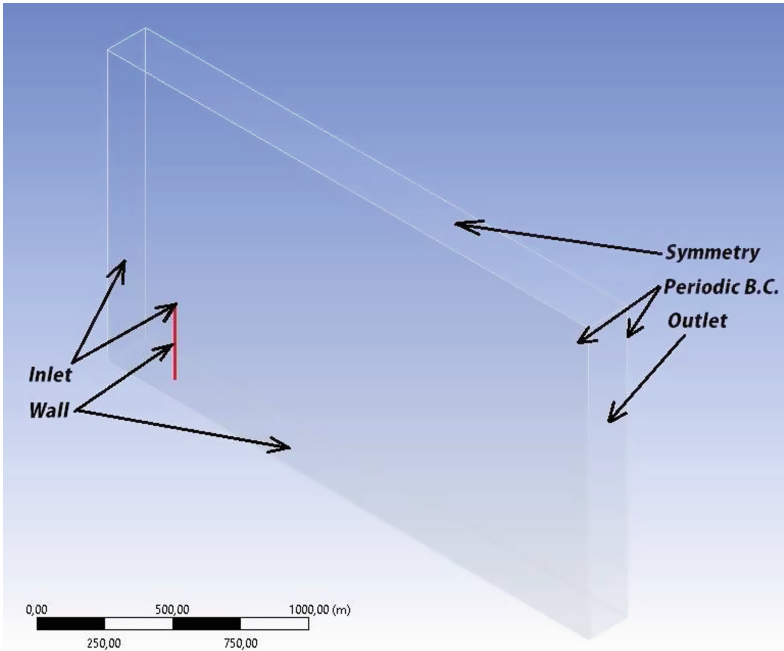


Fig. 3. Configuration of thermal power plant computational domain.

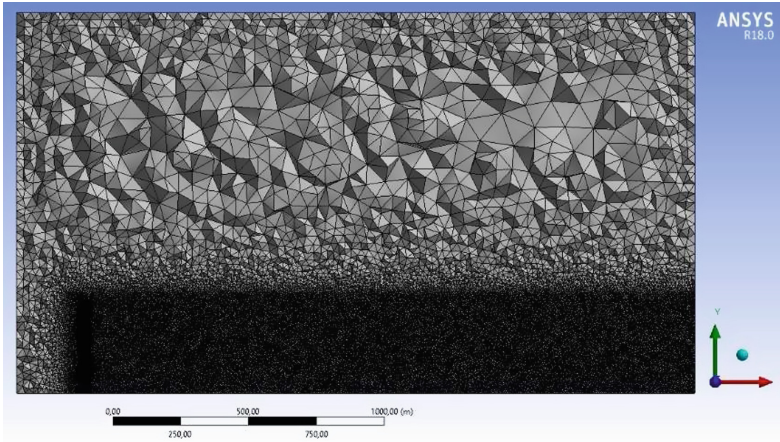


Fig. 4. Computational mesh

An unstructured grid was constructed. It was refined in the area of the pollution motion trajectory (See Fig. 4). Around the pipe, the grid size was 1 m, with 1.1 growth factor, in the remaining refined region the maximum grid size was 6 m. As a result, the computational grid consists of 822 056 nodes and 4 788 517 three-dimensional elements.

3.5 Flow Characteristics

To account for the boundary layer, the wind speed profile was described as follows: $v_x = v_{wind} \cdot (0.2371 \cdot \ln(Y + 0.00327) + 1.3571)$ [ms^{-1}]. In these calculations, the wind speed was 1.5 m/s. The velocity of pollution was 5 m/s. CO_2 was selected as a substance of emission. The influence of gravity force was taken into account. It was accepted that there is no chemical reaction between pollution and air.

3.6 Results

Figure 5 shows the distribution of CO_2 pollution concentration, visualized using the Volume Rendering option in ANSYS. Visually, the diffusion effect is observed with increasing distance from the source. The concentration was measured in mass fractions. Mass fraction of species is the mass of a species per unit mass of the mixture (e.g., kg of species in 1 kg of the mixture), i.e. dimensionless quantity. Figure 6 shows profiles of CO_2 distribution at different distances from the source (500, 1000, 1500, 2000 and 2200 [m]). Based on numerical results, it can be concluded that the CO_2 concentration reaches the surface of the earth at a distance of 2200 m from the stack. At a distance of 2200 m the emission concentration is spreading in the range from the ground surface to 420 m in height.

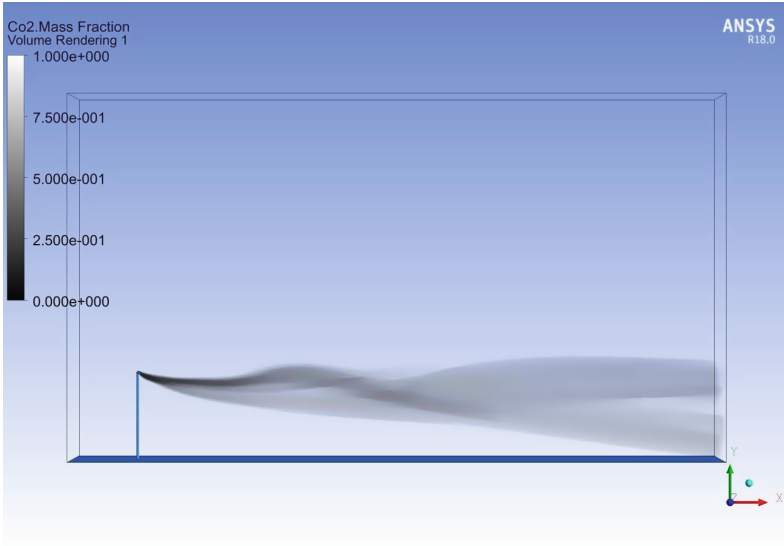


Fig. 5. The isosurface of CO_2 distribution

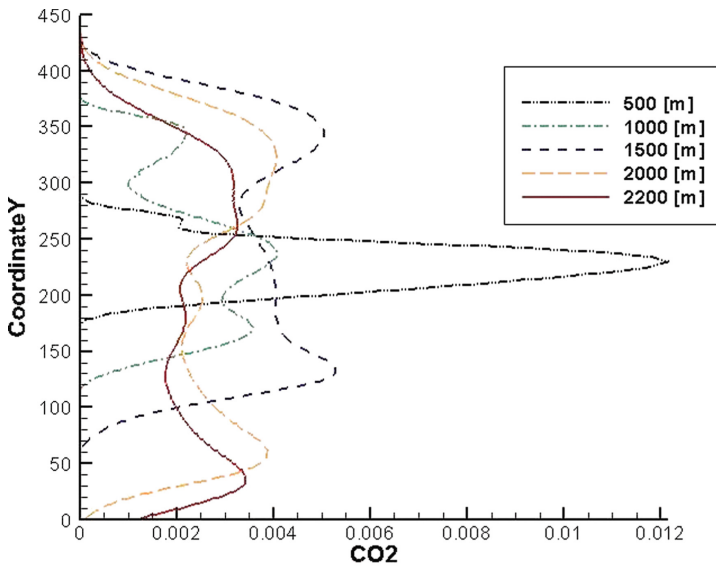


Fig. 6. CO_2 mass fraction profiles at various distances for chimney: 500, 1000, 1500, 2000, 2200 [m]

The Fig. 7 shows a CO_2 pollution distribution contour at the plane XY. Pollution settles on the ground surface at a distance of about 2220 m from the origin (i.e, 1970 m from the source).

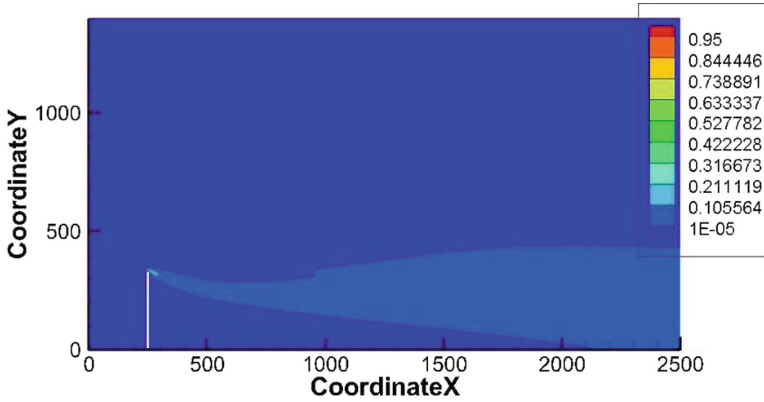


Fig. 7. The CO_2 mass fraction distribution contour at the center plane XY slice

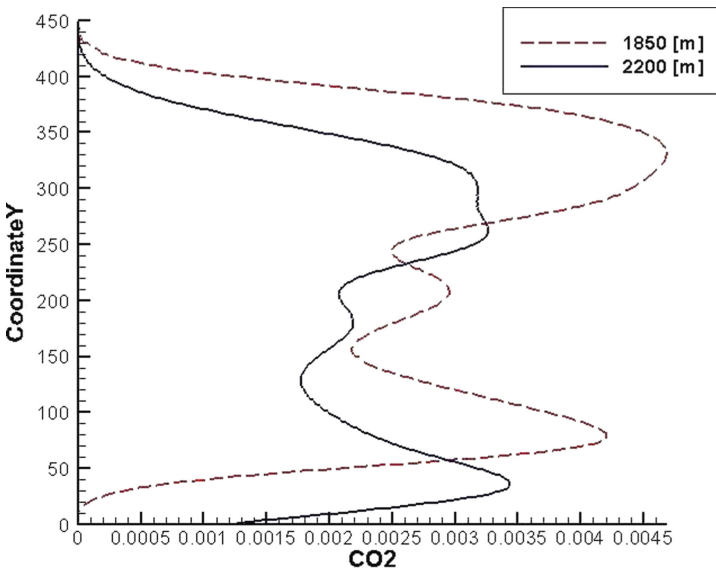


Fig. 8. CO_2 mass fraction profiles at various distances for chimney: 1850 and 2200 [m]

This is also confirmed by the following concentration distribution profiles at a distances of 1850 and 2200 m from the source (Fig. 8). At a distance of 1850 m, the concentration does not reach the ground and spreads at a height of about 20 m, while at a distance of 2200 m the concentration already reaches the ground. It can also be noted that the level of concentration decreases with increasing distance from the source: at a distance of 1850 m the maximum value of the pollution mass fraction is 0.0045, while at a distance of 2200 m the maximum value reached only 0.0035.

4 Conclusion

The purpose of this investigation was to study the dynamics of the emissions spread from energy objects. The computational fluid dynamics (CFD) techniques in modeling the pollution distribution from thermal power plant were considered. The mathematical model, turbulent model and numerical algorithm were tested using a test problem and gave a good match with the experimental data. The results obtained in this paper were closer to experimental, in comparison with the results of other authors. This was influenced by the quality of the grid: the unstructured and refined mesh gave a better result than the structured one. Carbon dioxide (CO_2) dispersion from a thermal power plant was simulated. The influence of gravity force was taken into account. To close the RANS equations was used the k-epsilon turbulent model. No additional dispersion model was applied. All simulations were performed by ANSYS Fluent. As a result, there was found a distance from the source at which the impurity settles on the ground surface. According to the obtained data, with increasing distance from the source, the concentration of pollution spreads wider under the influence of diffusion. The further the distance from the pipe then the lower the concentration. Thus, the obtained numerical data may allow in the future to predict the optimal distance from residential areas for constructing a TPP at which the emission concentrations will be at a safe level. These studies are useful for those who are interested in gas pollutant distribution in the atmosphere.

References

1. Issakhov, A., Baitureyeva, A.: Numerical modelling of a passive scalar transport from thermal power plants to air environment. *Adv. Mech. Eng.* **10**(10), 1–14 (2018)
2. Margason, R.J.: Fifty years of jet in crossflow research. In: AGARD Symposium on a Jet in Cross Flow, Winchester, UK. AGARD CP 534 (1993)
3. Kamotani, Y., Greber, I.: Experiments on turbulent jet in a crossflow. *AIAA J.* **10**, 1425–1429 (1972)
4. Fearn, R.L., Weston, R.P.: Vorticity associated with a jet in crossflow. *AIAA J.* **12**, 1666–1671 (1974)
5. Andreopoulos, J., Rodi, W.: Experimental investigation of jets in a crossflow. *J. Fluid Mech.* **138**, 93–127 (1984)
6. Krothapalli, A., Lourenco, L., Buchlin, J.M.: Separated flow upstream of a jet in a crossflow. *AIAA J.* **28**, 414–420 (1990)
7. Fric, T.F., Roshko, A.: Vortical structure in the wake of a transverse jet. *J. Fluid Mech.* **279**, 1–47 (1994)
8. Smith, S.H., Mungal, M.G.: Mixing, structure and scaling of the jet in crossflow. *J. Fluid Mech.* **357**, 83–122 (1998)
9. Su, L.K., Mungal, M.G.: Simultaneous measurement of scalar and velocity field evolution in turbulent crossflowing jets. *J. Fluid Mech.* **513**, 1–45 (2004)
10. Shan, J.W., Dimotakis, P.E.: Reynolds-number effects and anisotropy in transverse-jet mixing. *J. Fluid Mech.* **566**, 47–96 (2006)
11. Broadwell, J.E., Breidenthal, R.E.: Structure and mixing of a transverse jet in incompressible flow. *J. Fluid Mech.* **148**, 405–412 (1984)

12. Karagozian, A.R.: An analytical model for the vorticity associated with a transverse jet. *AIAA J.* **24**, 429–436 (1986)
13. Hasselbrink, E.F., Mungal, M.G.: Transverse jets and jet flames. Part 1. Scaling laws for strong transverse jets. *J. Fluid Mech.* **443**, 1–25 (2001)
14. Muppidi, S., Mahesh, K.: Study of trajectories of jets in crossflow using direct numerical simulations. *J. Fluid Mech.* **530**, 81–100 (2005)
15. Issakhov, A., Baitureyeva, A.: Numerical study of a passive scalar transport in lower atmosphere layer from thermal power plants. In: American Institute of Physics Conference Proceedings, vol. 1978, p. 470052 (2018). <https://doi.org/10.1063/1.5044122>
16. Muppidi, S., Mahesh, K.: Direct numerical simulation of passive scalar transport in transverse jets. *J. Fluid Mech.* **598**, 335–360 (2008)
17. Chochua, G., et al.: A computational and experimental investigation of turbulent jet and crossflow interaction. *Numer. Heat Transf. A* **38**, 557–572 (2000)
18. Acharya, S., Tyagi, M., Hoda, A.: Flow and heat transfer predictions for film-cooling. *Ann. NY Acad. Sci.* **934**, 110–125 (2001)
19. Issakhov, A.: Large eddy simulation of turbulent mixing by using 3D decomposition method. *J. Phys. Conf. Ser.* **318**(4), 1282–1288 (2011). <https://doi.org/10.1088/1742-6596/318/4/042051>
20. Issakhov, A.: Mathematical modeling of the discharged heat water effect on the aquatic environment from thermal power plant. *Int. J. Nonlinear Sci. Numer. Simul.* **16**(5), 229–238 (2015). <https://doi.org/10.1515/ijnsns-2015-0047>
21. Issakhov, A.: Mathematical modeling of the discharged heat water effect on the aquatic environment from thermal power plant under various operational capacities. *Appl. Math. Model.* **40**(2), 1082–1096 (2016). <https://doi.org/10.1016/j.apm.2015.06.024>
22. Issakhov A., Baitureyeva A.R.: Numerical simulation of a passive scalar transport from thermal power plants. In: American Institute of Physics Conference Proceedings, vol. 1836, p. 020019 (2017). <https://doi.org/10.1063/1.4981959>
23. Issakhov, A., Baitureyeva, A.R.: Numerical simulation of a pollutant transport in lower atmosphere layer from thermal power plants. *WSEAS Trans. Fluid Mech.* **12**, 33–42 (2017). Article no. n4
24. Ferziger, J.H., Peric, M.: *Computational Methods for Fluid Dynamics*, 3rd edn. Springer, Heidelberg (2013). <https://doi.org/10.1007/978-3-642-56026-2>
25. Issakhov A., Mashenkova, A.: Numerical study for the assessment of pollutant dispersion from a thermal power plant under the different temperature regimes. *Int. J. Environ. Sci. Technol.* 1–24 (2019). <https://doi.org/10.1007/s13762-019-02211-y>
26. Issakhov, A., Bulgakov, R., Zhandalet, Y.: Numerical simulation of the dynamics of particle motion with different sizes. *Eng. Appl. Comput. Fluid Mech.* **13**(1), 1–25 (2019)
27. Chung, T.J.: *Computational Fluid Dynamics*. Cambridge University Press, Cambridge (2002)
28. ANSYS Fluent Theory Guide 15, ANSYS Ltd. (2013)
29. Ajersch, P., Zhou, J.M., Ketler, S., Salcudean, M., Gartshore, I.S.: Multiple jets in a crossflow: detailed measurements and numerical simulations. In: International Gas Turbine and Aeroengine Congress and Exposition, ASME Paper 95-GT-9, pp. 1–16, Houston, TX (1995)
30. Keimasi, M.R., Taeibi-Rahni, M.: Numerical simulation of jets in a crossflow using different turbulence models. *AIAA J.* **39**(12), 2268–2277 (2001)